

Late Holocene (~3 ka) Paleoclimatic Records from Baspa Valley, NW Himalaya: A Multi-Proxy Approach

Firoz Khan^{1,2,3}, Narendra Kumar Meena^{1,2*}, Yaspal Sundriyal^{1,4} and Rajveer Sharma⁵

¹Department of Geology, H.N.B. Garhwal University, Srinagar-246174 (UK), India

²Wadia Institute of Himalayan Geology, 33 G.M.S. Road, Dehradun-248001(UK), India

³Atal Bhujal Yojana, Kurukshestra-136119(HR), India

⁴Department of Geology, Doon University, Dehradun-248012(UK), India

⁵Inter University Accelerator Center (IUAC), New Delhi-110067, India

(*Corresponding Author, E-mail: narendes@gmail.com)

Abstract

We investigated a 83-cm-thick fluvio-glacial sedimentary profile from Baspa Valley, Central Himalaya, where monsoonal precipitation and glacial deposits are well preserved. We use a multi-proxy strategy to reconstruct Late-Holocene climatic variability in this region, including carbon isotope, environmental magnetism, total organic carbon, and AMS Carbon-14 dating. These multi-proxy data showed alternate warm and cool climatic phases that govern glacial snow melting and advancement, respectively. The current study revealed that the climate was warm and moist (deglaciation phases) from 2.9 to 1.5 ka and 1 to 0.5 ka. The warm and moist conditions in this area are characterised by depleted carbon isotope values, high organic production, and high magnetic mineral concentrations. The Indian monsoon conditions were very intense during this time period. Cold and dry climatic conditions (glacial phase) were recorded between 1.5 and 1 ka, as shown by carbon isotope enrichment, lower organic production, and low magnetic mineral concentrations. During this period, weak monsoonal conditions were observed in the Baspa region, Northwest Himalayan region.

Keywords: Palaeoclimate, Environmental Magnetism, Carbon Isotope, AMS 14C Dating, Baspa Valley, NW Himalaya

Introduction

Glacial deposits are one of the most reliable indicators of climate change. The short-term changes in snow/ice melting occur owing to warming in the climate and this climate signature is preserved in the form of annual layers in the glacial lakes and glacial outwash deposits whereas the long-term changes in the glaciers are reflected in the moraines deposits (Shukla *et al.*, 2020). Recent studies on the moraine and glacial lake deposits shows that the quality and reproducibility of the glacial variations during the Holocene have significantly increased in the Himalayas (Shukla *et al.*, 2020; Meena *et al.*, 2022; Lone *et al.*, 2022; Khan *et al.*, 2022; Khan, 2023; Sagwal *et al.*, 2023; Meena *et al.*, 2024). Hence, high-resolution climatic studies using glacial deposits are very significant to understand the glacial/deglacial patterns in the Himalayas related to climate change.

The Himalaya plays a significant role in influencing the climate across the northern belt of the Indian sub-continent. Long-term climatic change is influenced by the unique characteristics of Indian orography in the Northwestern Himalaya, which alters the

pattern of precipitation over the area (Shekhar *et al.*, 2010). Mid-latitude Westerlies (MLW) and the Indian Summer Monsoon (ISM) are the principal precipitation producers in the Himalayas. On a millennial to decadal timescale, the ISM and MLW variations have historically governed the changes in Himalayan glaciers (Benn and Owen, 1998). The precipitation trend normally declines from East to West because the ISM trough gets smaller as it advances towards the west along the Himalayan mountain range (Bookhagen and Burbank, 2010). The eastern Himalaya receives precipitation that is primarily brought on by the ISM. In the western Himalaya, MLW contributes about 2/3rd of the annual precipitation in the form of high-altitude snowfall during winters, with the remaining 1/3rd coming from precipitation primarily due to ISM in the summer (Armstrong, 2010). It is difficult to comprehend the climatic mechanisms that generate natural catastrophes in the Himalayan area as a result of these complicated weather phenomena (Rana *et al.*, 2021a, b; Agarwal *et al.*, 2022). Since the first climatic study at Baspa (Sangla) Valley, Northwest Himalaya (Ganjoo and Koul, 2005), several investigations have been performed to reconstruct Late Quaternary to Holocene climate (Chakraborty *et al.*, 2006; Ranhotra and Bhattacharyya, 2010; Ranhotra *et al.*, 2018; Khan *et al.*, 2022; Khan, 2023) and glaciers fluctuation (Bhattacharyya *et al.*, 2006; Draganits *et al.*, 2014a, b; Dutta *et al.*, 2018; Ranhotra *et al.*, 2022). The Karu, Jorya, Janapa, Naradu, Magsu, and Shushang are the

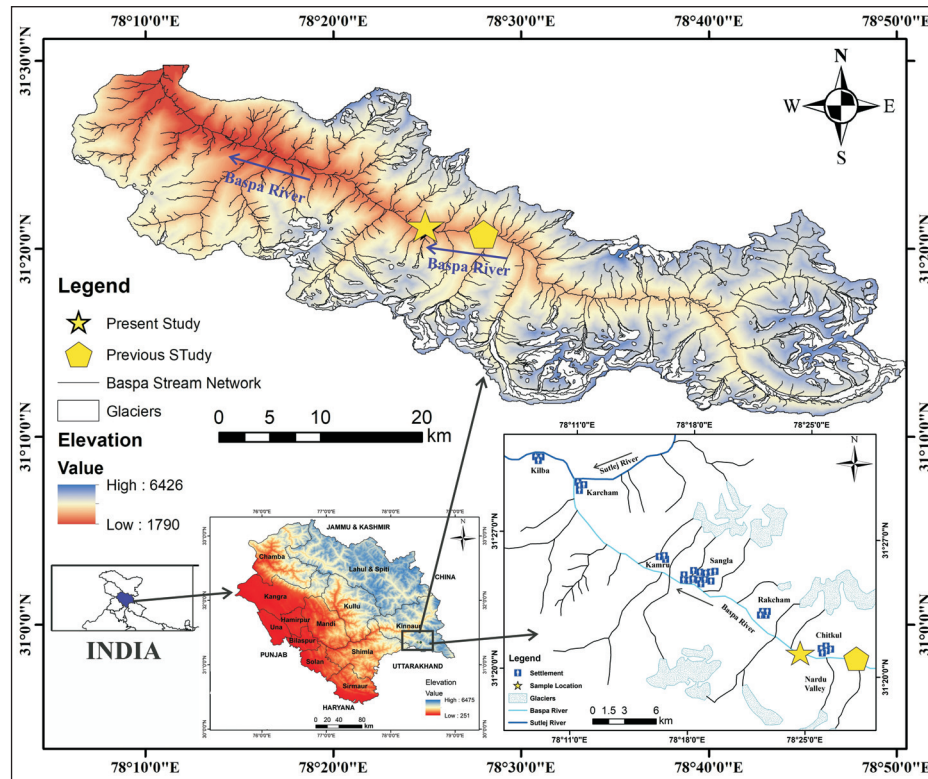


Fig.1. Digital elevation model of the Baspa Valley showing the study area, drainage network and glacial bodies.

primary glaciers of the Baspa Valley, and they are located between altitudes of 4000 to 6200 m above mean sea level (amsl). According to various high-resolution palaeorecords in the Himalayas, temperature and precipitation conditions in the Himalayas are strongly impacted by fluctuations in insolation on the orbital and decadal time scales (Gupta *et al.*, 2005).

This study area is very crucial for understanding glacial-monsoon system dynamics as it is located in a transitional climate zone influenced by both the ISM and MLW. The present study attempts to document the glacial/deglacial patterns in a high-altitude Himalayan region owing to climate change using fluvio-glacial sedimentary deposits. It is essential to comprehend the climate role in driving the glacial/deglacial processes in the transitional climate zone basin of the Northwest Himalaya. The main goal of the present study is to understand the multifaceted glacial-climate system by reconstructing climate variations in the Baspa valley, Kinnaur during Late Holocene.

Study Area

The study area lies in Sangla town of Baspa Valley which is located on the southern fringe of the Tibetan Plateau at latitude 31.35°N and longitude 78.42°E and at an altitude of ~3450 m amsl (Fig.1). The Baspa River rises from the Arsomang and Baspa glaciers and joins the Sutlej River in Karcham (1890 m amsl). It covers an area of 1100 km² with elevation ranges between 1770 to 6465 m amsl. The sediment deposited in this region owing to the glacial melt water or the damming in the Baspa Valley during the Late Quaternary period (Ganjoo and Kaul, 2005; Draganits *et al.*, 2014a, b; Dutta *et al.*, 2018).

The research area is situated in the Higher Himalaya and is mostly made up of rocks from the Haimanta and Vaikrita Groups.

The Vaikrita Group (Early to Middle Proterozoic) comprises gneiss, sillimanite-bearing schist, migmatite, and quartzite whereas the Haimanta Groups of rocks are composed of greenish shale, grey phyllites, quartzite, and carbonaceous slate (Bhargava and Bassi, 1998). The South Tibetan Detachment fault, also known as the Sangla Detachment fault locally, separates the Higher Himalayan Crystalline and Tethyan Sedimentary Sequence (Vannay *et al.*, 2004). Temperate broad-leaved and coniferous plants dominate the vegetation cover. At a height of >3400 m amsl, the coniferous forest merges with the sub-Alpine Forest, whereas the broadleaved-conifer forest grows at a lower elevation of 2600 m amsl (Ranhotra *et al.*, 2018).

Materials and Methods

Sampling and Lithology of the Sedimentary Archive

In 83 cm of fluvio-glacial outwash deposits, 82 samples were collected from Chitkul village, Kinnaur, Himachal Pradesh at an interval of 1 cm for multi-proxy analyses. The exposed stratigraphy of the profile is dominated by silty clay layers with a distinct colour. The litho-stratigraphy of the profile is represented in figure 2.

AMS ¹⁴C Dating

To obtain the chronology of the fluvio-glacial sediment profile, AMS ¹⁴C dating was conducted at the IUAC, New Delhi. For AMS ¹⁴C dating, four samples were selected i.e., 2-3, 25-26, 76-77, and 82-83 cm. The HCL-NaOH-HCL (acid-base-acid) standard technique was used to pre-treat the sediment samples (Sharma *et al.*, 2019). The dates have been calibrated using Bacon software and IntCal13 with 95% accuracy (Blaauw and Christen, 2013).

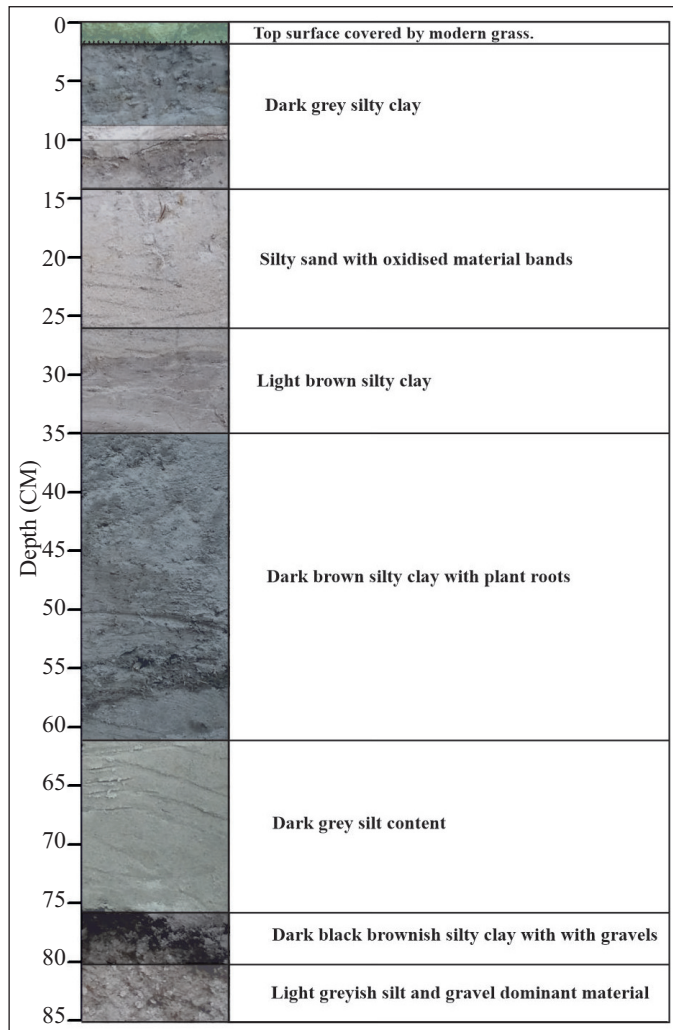


Fig.2. Lithostratigraphy of the sedimentary section at Chitkul (CTL-1) Village, Baspa valley, Kinnar, Himachal Pradesh.

Environmental Magnetism

41 samples for environmental magnetism was analysed at the Wadia Institute of Himalayan Geology, Dehradun. The air-dried sediment samples were crushed with an agate pestle-mortar before being carefully packed into a standard non-magnetic 10 cm³ styrene container for environmental magnetic analysis. Using a dual frequency Bartington MS2B laboratory sensor, the χ_{lf} was measured at a low frequency (460 Hz) and the χ_{hf} at a high frequency (4600 Hz). ARM was measured in an alternating field of 100 mT peak field superimposed over 0.1 mT DC field using a Molspin AF Demagnetizer, and remanence was measured using a Mini spin Fluxgate Spinner Magnetometer. The Isothermal Remanent Magnetization (IRM) was computed using an ASC Model IM-10 Impulse Magnetizer imparted at forward and back fields, and remanences were calculated using a Mini spin Fluxgate

Spinner Magnetometer. The remaining isothermal remnant magnetization parameters of the mineral were calculated using the following formulas: Saturation Isothermal Remnant Magnetization (SIRM) was applied at 1000 mT, Soft-IRM by $0.5 \times (\text{SIRM} - \text{IRM}_{20\text{mT}})$, HIRM by $0.5 \times (\text{SIRM} + \text{IRM}-300\text{mT})$, and S-ratio by $\text{IRM}-300\text{mT}/\text{SIRM}$.

Isotopic Analysis and Total Organic Carbon

41 samples for each $\delta^{13}\text{C}$ and TOC were analysed at the Wadia Institute of Himalayan Geology, Dehradun. ~2 g of air-dried fine powdered sediment samples were treated with 0.6 N HCl in order to remove the carbonate for carbon isotope ($\delta^{13}\text{C}$) measurement (Agrawal *et al.*, 2015). Following HCl treatment, the samples were centrifuged at 3000 rpm while being washed with Milli-Q water to remove the acids and other soluble salts. The sediment samples were then dried in an oven at 50 °C and ~0.5 to 15 mg of sediments were packed in Tin capsules for combustion during the $\delta^{13}\text{C}$ analysis. The CO₂ was measured using a continuous Flow Isotope Ratio Mass Spectrometer (CF-IRMS) combined with a Flash Elemental Analyzer. Calibration was made by IAEA and ACA standards for the $\delta^{13}\text{C}$. The measured $\delta^{13}\text{C}$ findings were expressed with Vienna PeeDee Belemnite (VPDB) and measured with an accuracy of 0.1‰ (2σ).

~1-2 g of the bulk dried sediment were cleaned with 1N HCl and Milli-Q water for the TOC measurement, and they were subsequently dried at a temperature of 900°C into SSM-5000A. The SSM-5000A analyzer was then used to test for inorganic carbon (IC) and total carbon (TC) at temperatures of 200°C and 900°C, respectively, using ~10 mg sediment samples. The analyzer produces findings that are the sum of integrated m/z 44, 45, and 46 signals that are measured in CFIRMS and represented as weight percent (wt%). The relationship between TC, IC, and TOC is: TOC = TC - IC.

Results

AMS ^{14}C Dating and Age-Depth Model

Four sediment samples from the Inter-University Accelerator Centre (IUAC), New Delhi, were examined to determine the chronology (Table 1). The obtained ^{14}C ages are 446 ± 24 yr BP, -468 ± 25 yr BP and 2774 ± 60 yr BP from the depth of 2-3 cm, 76-77 cm, and 82-83 cm, respectively (Table 1). One sample (25-26 cm) could not be dated due to insufficient amount of carbon content while another sample (76-77) indicates age inversion and is considered an outlier. The radiocarbon ages are calibrated using bacon software with two sigma error and 95% confidence and prepared the age-depth model (Fig.3). The two calibrated radiocarbon ages i.e., 502.5 and 2895 yr BP are interpolated to obtain the chronology and has been used for interpretation from the entire sedimentary profile. The sediment accumulation rate of the fluvio-glacial sequence is ~0.29 mm/yr.

Table 1: AMS ^{14}C dating ages of the fluvio-glacial deposits from the Baspa Valley, Northwest Himalaya calibrated by Bacon software with two sigma error and 95% accuracy (Blaauw and Christen, 2013)

Lab Number	Depth (cm)	Sample Type	AMS ^{14}C age (yr BP)	Calibrated age (cal yr BP)	Error (2σ)	Midpoint calibrated age (cal yr BP)
IUACD#19C2794	2-3	Organic material	446 ± 24	475-530		502.5
IUACD#19C2796	76-77	Organic material	-468 ± 25	-		Modern Age
IUACD#19C2797	82-83	Organic material	2774 ± 60	2750-3040		2895

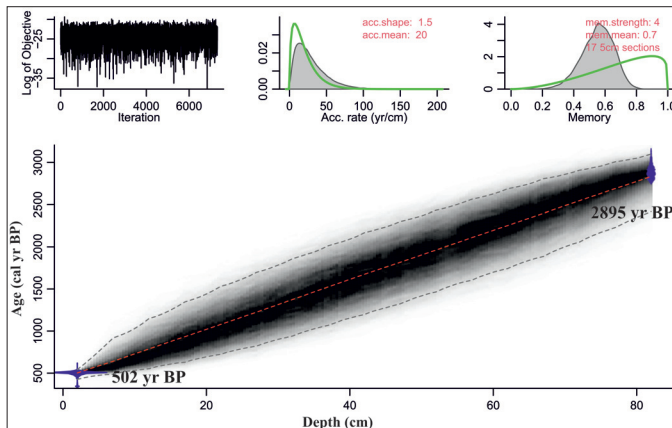


Fig.3. Age-depth model of the studied profile using Bacon software.

Stable isotope ($\delta^{13}\text{C}$) and Total organic carbon (TOC)

The $\delta^{13}\text{C}$ values of the sediment section indicate substantial variation with depth. The $\delta^{13}\text{C}$ values vary from -28.17 to -21.71‰. From the bottom of the section, the $\delta^{13}\text{C}$ value is -26.5‰ which depleted the maximum to -28.17‰ at the depth of 74 cm (Fig.4). The $\delta^{13}\text{C}$ data shows maximum enrichment of -21.71‰ around the 10 cm depth from the section and then shows depletion of -26.45‰ at depth of 6 cm (Fig.4). The TOC values vary between 0 and 5.9% in the sediment profile (Fig.4). The sedimentary profile indicates high TOC at depth of 78 cm which gradually decreases from 78 to 74 cm and progressively increases from 74 to 34 cm. The TOC is low between 34 to 26 cm and then gradually increases from 26 to 2 cm (Fig.4).

Environmental Magnetism

Environmental magnetism is a vigorous proxy in lake sediments to understand the magnetic characteristics of natural materials, which depend on the creation, transport, deposition, as well as transformation of magnetic minerals regulated by the environmental condition and geomorphic processes (Basavaiah and Khadkikar, 2004; Rawat *et al.*, 2015b; Basavaiah *et al.*, 2022). The

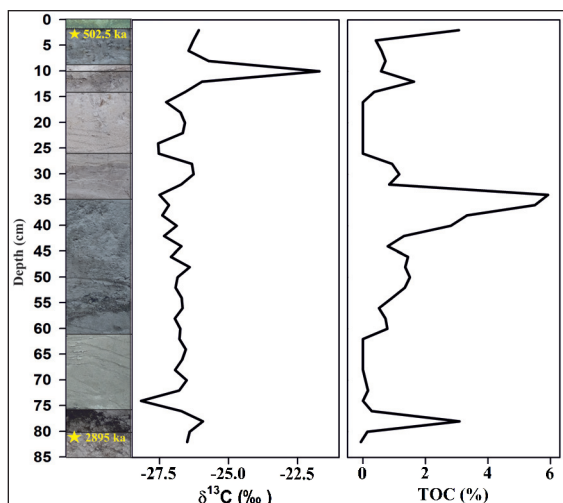


Fig.4. Down depth variation in the Carbon isotope and total organic carbon from Baspa Profile (CTL-1), Kinnaur, Himachal Pradesh.

inter-parametric scatter plots of the magnetic data from the sedimentary profile (CTL-1) are displayed in figure 5. Correlations (r^2) are observed between χ_{lf} and S-Ratio; Bcr and S-Ratio; χ_{lf} and χ_{ARM} ; SIRM and χ_{lf} ; S-Ratio and $\delta^{13}\text{C}$; χ_{lf} and Bcr; χ_{lf} and TOC; $\delta^{13}\text{C}$ and TOC are $\sim 0.24, 0.28, 0.55, 0.43, 0.46, 0.13, 0.25, 0.44$, and 0.01, respectively. χ_{lf} values vary between 0.3 and 0.9 ($10^{-8} \text{ m}^3 \text{ kg}^{-1}$), ARM from 0.9 to 9 ($10^{-8} \text{ m}^3 \text{ kg}^{-1}$), S-Ratio from -1.03 to -0.68, SIRM from 31 to 200 ($10^{-5} \text{ Am}^2/\text{kg}$), Soft-IRM from 15 to 94, HIRM from 0 to 20.35, Bcr from 10 to 49 mT (Fig.6).

Discussion

The present study demonstrated the climate-glacial dynamics using multi-proxy ($\delta^{13}\text{C}$, TOC and Environmental Magnetism) analysis in the fluvio-glacial sediment deposits in the transitional climate zone from the Baspa Valley, NW Himalaya. The three climatic zones were identified from the Baspa profile i.e., ~ 3 to 1.5 ka, ~ 1.5 to 1 ka and ~ 1 to 0.5 ka (Fig.6). Fluvio-glacial and lacustrine sediments accumulated from the blocking of the Baspa River by a rock avalanche during the Late Quaternary (Ganjoo and Koul, 2005). The sediment accumulation rate of the fluvi-glacial sequence is approximately 0.29 mm/year. Recent research analyzed high sedimentation rates in lakes across various hydroclimate zones in northern India (Diwate *et al.*, 2021). During the Middle to Early Holocene, the glaciers were present at an elevation of ~ 3500 m amsl within the Baspa Valley (Ranhotra and Bhattacharyya, 2010). The glacial bodies retreated to the upper reaches of the Baspa Valley during this time, and glacial meltwater is the main source of feeding lakes during the Late-Pleistocene to Late Holocene time (Draganits *et al.*, 2014a).

According to a scatter plot between the χ_{lf} and χ_{ARM} correlation in the present study, superparamagnetic/single domain size particles are associated with a greater concentration of magnetic susceptibility (Rawat *et al.*, 2015b), while the bulk susceptibility has been influenced by a little fluctuation in magnetic grains, as evidenced by the correlation between χ_{lf} and SIRM (Fig.5; Liu *et al.*, 2012; Sharma *et al.*, 2020). The hematite and goethite magnetic hard minerals are regulated by the rise in coercivity, according to the correlation between Bcr and S-Ratio (Fig.5; Rawat *et al.*, 2015b). Hematite is transformed into magnetite during the fermentation process in a warm and humid environment as a result of magnetic enrichment caused by the breakdown of organic materials (Fig.5).

Zone 1: ~ 3 to 1.5 ka

During ~ 3 to 1.5 ka, the mineral magnetic proxy parameters such as χ_{lf} , SIRM, HIRM, S-Ratio and Bcr shows increasing trend which suggested an increase in magnetic minerals concentrations under a warm-wet climate (Fig.6). The magnetizability of sediments that have undergone weathering and pedogenic processes is revealed via χ values (Basavaiah and Khadkikar, 2004). Therefore, high susceptibility (χ) values indicates the high occurrence of iron minerals is roughly proportional to concentration of strongly magnetic minerals like magnetite (Oldfield, 1991; Meena *et al.*, 2011). Higher values of HIRM signify an abundance of anti-ferromagnetic minerals (high coercivity minerals) (Liu *et al.*, 2012). S-Ratio, a measure of coercivity that takes into account both mineralogy and grain size, is a ratio of saturated to non-saturated minerals (Oldfield, 1991). Hence, higher values of S-

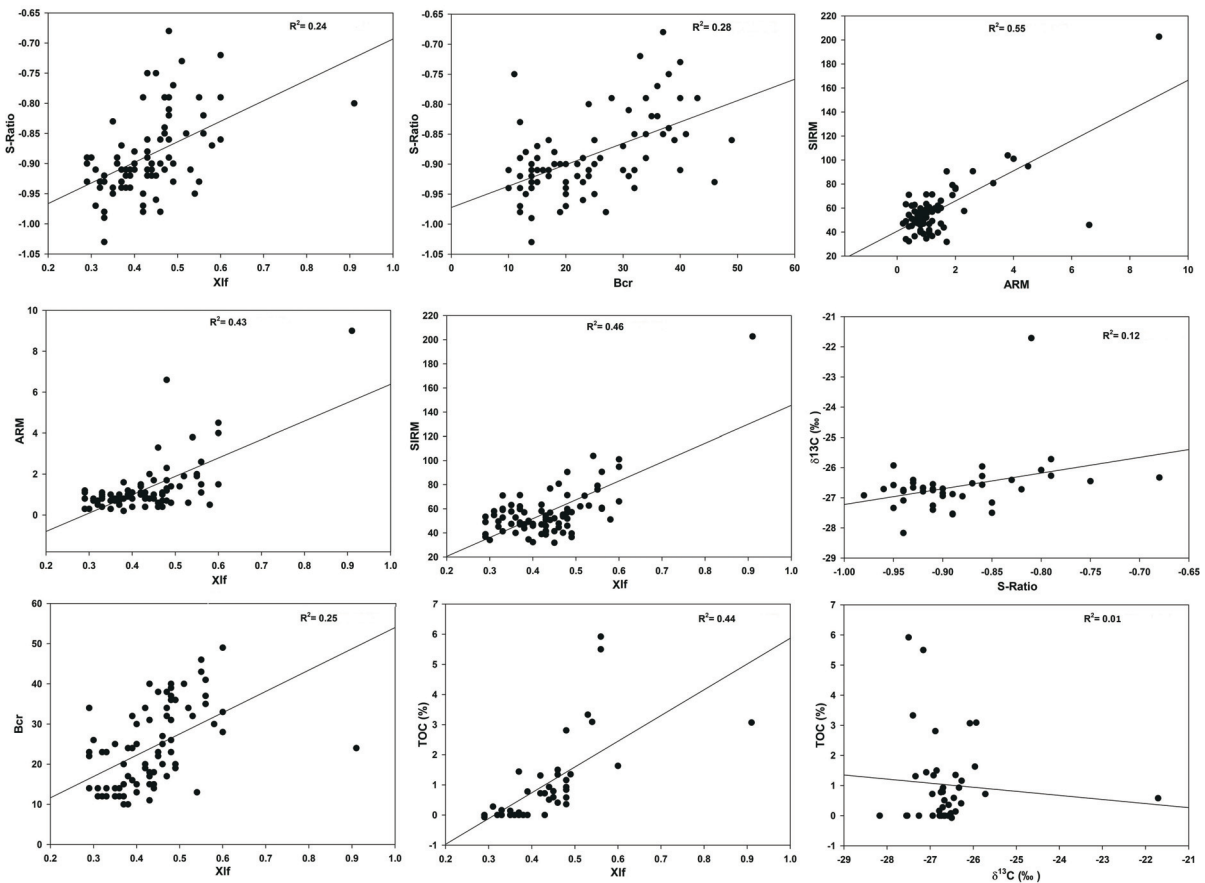


Fig.5. Scatter plots (r^2) indicate the relation between the various parameters of mineral magnetic parameters with the carbon isotope ($\delta^{13}\text{C}$) and total organic carbon (TOC) data of the studied sedimentary archive from the Baspa valley, Kinnaur, NW Himalaya.

Ratio are dominated by magnetite and titanomagnetite like minerals with low coercive forces (Basavaiah *et al.*, 2022). The SIRM must be reduced to zero in order to achieve the remanent coercivity (Bcr), which is frequently used to differentiate between various magnetic minerals and particle sizes (Thompson *et al.*, 1980). The high Bcr values indicate high coercivity in antiferromagnetic minerals like hematite (Rawat *et al.*, 2015b). A strong connection exists between the erosional processes and rising detrital titano-magnetite concentration, as shown by comparatively greater values of χ and S-ratio (Basavaiah and Khadkikar 2004). The observed increased concentrations of magnetic minerals present in the Baspa sequence strongly suggest that there has been a significant and vigorous soil flux originating from the catchment area. This phenomenon appears to be a result of rapid erosion taking place in the region. Furthermore, this erosion is indicative of broader climatic patterns, reflecting periods of climatic warming followed by phases of cooling. The relationship between the soil flux and the concentrations of these magnetic minerals serves as compelling evidence of the environmental changes at play. The $\delta^{13}\text{C}$ data from the studied section range between -28.17 to -21.71‰ which signifies the C3 plants vegetation. The TOC value increased between ~2.9 to 1.5 ka, suggesting high organic productivity (Fig.6). It has been suggested that the mineral magnetic parameters show high magnetic mineral concentrations and high organic productivity in the fluvo-glacial deposits due to the intense monsoonal climatic conditions. But at bottom of the profile, around 2.8 ka, sudden depletion in the $\delta^{13}\text{C}$ as well as increased value of TOC and high concentrations of magnetic minerals are observed

which suggested warm and moist climatic conditions (Fig.6). Khan *et al.* (2022) previously reported warming in Baspa Valley, based on peat records. Similar records from peat deposits also found in Chandra Valley (Rawat *et al.*, 2015a, b), and Ladakh (Maurya *et al.*, 2022; Sagwal *et al.*, 2023) indicate a warmer climatic phase. This warming has also been captured in the paleolake deposits studied by Chakraborty *et al.* (2006) from Sangla Valley, Kinnaur. Various Himalayan lakes records (Hou *et al.*, 2017; Rawat *et al.*, 2021; Sharma *et al.*, 2020) and Tibetan lakes (Liu *et al.*, 2009; Ji *et al.*, 2005) also observed warm and humid climatic conditions which suggested deglacial phase during this period.

Zone 2: 1.5 to 1 ka

During ~1.5 to 1 ka, χ_{lf} , SIRM, and HIRM values decreases which indicates a reduction in the magnetic minerals concentrations (Fig.6). The χ_{ARM} shows the decreasing trend and it estimates the concentration of stable single domain ($0.025 \mu\text{m} < d < 0.05 \mu\text{m}$) ferrimagnetic minerals (magnetite) with fine grain, which are most abundant near the superparamagnetic/ stable single domain boundary and least abundant in coarser multidomain grains (magnetite; $d > 10 \mu\text{m}$) (Oldfield, 1991; Liu *et al.*, 2012). A decreasing trend of HIRM signifies a lower concentration of high coercivity anti-ferromagnetic minerals (Rawat *et al.*, 2015b). An increase in hard anti-Fe magnetic component (hematite) with a relatively large coercive force is also predicted by decreasing values of S-Ratio during this phase (Fig.6; Basavaiah *et al.*, 2022). Hence, a decrease in the χ_{lf} , χ_{ARM} , and S-ratio parameters indicates low

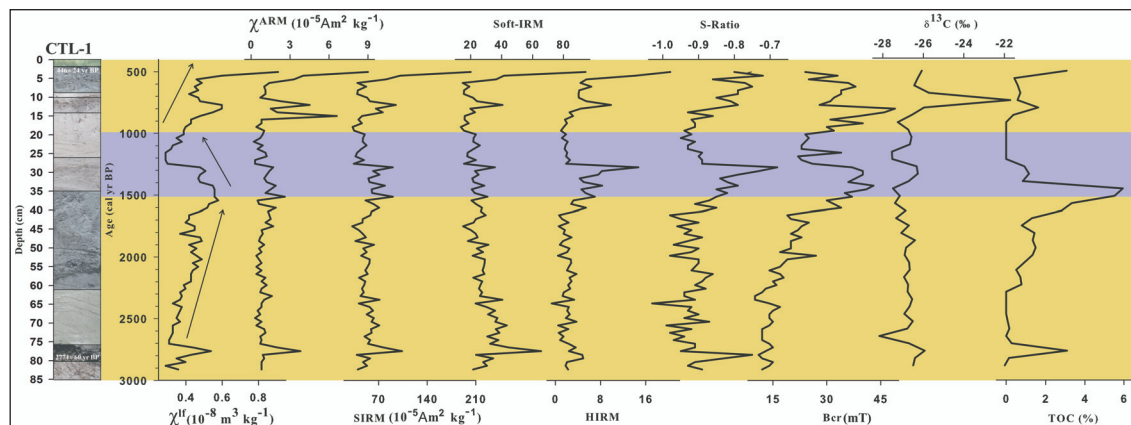


Fig.6. Compilation of the multi-proxy data viz. environmental magnetic parameters *i.e.*, χ_{lf} , χ_{ARM} , SIRM, Soft-IRM, HIRM, S-Ratio, Bcr and biochemical data *i.e.*, Carbon Isotope ($\delta^{13}\text{C}$), total organic carbon (TOC) data of Baspa sequence from NW Himalaya.

input of detrital sediments which signifies the cold and dry environmental conditions. These observations are also supported by the $\delta^{13}\text{C}$ and TOC proxy data (Fig. 6). The $\delta^{13}\text{C}$ has been enriched and an abrupt decrease in TOC values shows low organic productivity which signifies the cold and dry climatic scenario during this phase (Fig. 6). Around 1.3 ka, we observe a sudden spike in all the proxies which is an evidence of a short phase of warm climate (Fig. 6). Between ~1.5 to 1 ka, peat records from Baspa Valley (Khan *et al.*, 2022; Khan, 2023) from Central Himalaya and decreasing Pangong Tso Lake level (Hou *et al.*, 2017) suggest cold and dry climatic conditions. Similarly, Sharma *et al.* (2020) also reported cold and dry climatic conditions during this phase based on the pollen data from Ladakh Himalaya.

Zone 3: 1 to 0.5 ka

During 1 to 0.5 ka, the magnetic parameters like χ_{lf} , SIRM, HIRM, and Soft-IRM all show a considerable rise showing increased magnetic minerals concentration suggesting the warming in the environmental conditions (Fig. 6). The similar pattern is followed by χ_{ARM} , which demonstrates the existence of single domain grains containing ferromagnetic materials. According to HIRM, "Hard" refers to the relative abundance of high coercivity minerals like hematite in a combination of ferrimagnetic minerals (minerals that resemble magnetite), with greater HIRM indicating the predominance of antiferromagnetic minerals (Liu *et al.*, 2012). An increasing trend in S-Ratio confirms the presence of magnetite minerals (Basavaiah *et al.*, 2022). The depletion in $\delta^{13}\text{C}$ ratio and high organic productivity also evidence the warm climatic scenario of the Baspa Valley during this time (Fig. 6). But decrease magnetic mineral concentrations, enrichment in $\delta^{13}\text{C}$ and low organic productivity has been observed around 700 yr BP which suggested a cold-dry climate (Figure 6). Similar findings were also reported from the Sithikher Bog (Chauhan *et al.*, 2000), Parvati Valley (Chauhan, 2006), Chandra Valley (Rawat *et al.*, 2015a, b), and Triloknath Lake (Bali *et al.*, 2017) between ~1 to 0.5 ka from Himachal Pradesh, Northwest Himalaya which suggested warm and humid climate. Recent finding from the Anshupa Lake in core monsoon zone (Palar *et al.*, 2025) and Sherla Lake in Haryana (Kaushik *et al.*, 2025) were also supports the present finding from the Baspa Valley. Furthermore, the Dasuopu ice core records from the southern Tibetan Plateau also reflect this warming during this time period (Yang *et al.*, 2007).

Conclusions

Multi-proxy data on the fluvio-glacial sedimentary record from the Baspa valley, Kinnaur, Northwest Himalaya indicate palaeoclimatic changes during the last 3 ka. The multi-proxy data suggest warm-wet climatic conditions between ~3 to 1.5 ka and ~1 to 0.5 ka, coeval with the deglaciation phase in the NW Himalaya. The study indicates intense monsoonal activities during this time period. The present study also indicates cold-dry environmental conditions from 1.5 to 1 ka, which supported advancement in the Himalayan glacial regions. The Baspa sequence's increased magnetic (ferrimagnetic) mineral concentrations during ~3 to 1.5 ka and ~1 to 0.5 ka, imply high flux from catchment soil in response to fast erosion, which offers evidence of climatic warming and reduced concentration of magnetic minerals between ~1.5 to 1 ka inferred cold and dry climatic condition. The increasing concentration of anti-ferromagnetic minerals from ~1 to 0.5 ka suggested warm and moist climatic conditions in the Baspa valley, NW Himalaya.

Authors' Contributions

FK: Investigation, Conceptualization, Methodology, Writing - Original Draft, Software. **NKM:** Visualization, Supervision, Reviewing and Editing. **YS:** Visualization, Supervision, Reviewing and Editing. **RS:** Visualization, Reviewing and Editing, Formal Analysis.

Conflict of Interest

The authors declare that there is no conflict of interest.

Acknowledgments

This is Ph.D. work of Dr. Firoz Khan. The Director, Wadia Institute of Himalayan Geology (WIHG) was acknowledged by the authors for providing the required lab resources. For offering a university research fellowship, FK expressed gratitude to H.N.B. Garhwal Central University, Srinagar, Uttarakhand. FK also acknowledged Dr. Pranaya Diwate, Assistant Professor at MGM University in Aurangabad, Dr. Sonu Jaglan, Assistant Professor, Department of Higher Education, Haryana for their assistance throughout this study.

References

- Agarwal, S., Kumar, V., Kumar, S., Sundriyal, Y., Bagri, D.S., Chauhan, N., Kaushik, S., Khan, F. and Rana, N. (2022). Identifying potential hotspots of land use/land cover change in the last 3 decades, Uttarakhand, NW Himalaya. <https://doi.org/10.31223/X5VK9F>
- Agrawal, S., Srivastava, P., Meena, N.K., Rai, S.K., Bhushan, R., Misra, D.K. and Gupta, A.K. (2015). Stable ($\delta^{13}\text{C}$ and $\delta^{15}\text{N}$) isotopes and Magnetic Susceptibility record of late Holocene climate change from a lake profile of the northeast Himalaya. *Jour. Geol. Soc. India*, v. 86, pp. 696-705.
- Armstrong, R.L. (2010). The glaciers of the Hindu Kush-Himalayan region: a summary of the science regarding glacier melt/retreat in the Himalayan, Hindu Kush, Karakoram, Pamir, and Tien Shan mountain ranges. International Centre for Integrated Mountain Development (ICIMOD).
- Bali, R., Khan, I., Sangode, S.J., Mishra, A.K., Ali, S.N., Singh, S.K., Tripathi, J.K., Singh, D.S. and Srivastava, P. (2017). Mid-to late Holocene climate response from the Triloknath palaeolake, Lahaul Himalaya based on multiproxy data. *Geomorphology*, v. 284, pp. 206-219.
- Basavaiah, N. and Khadkikar, A.S. (2004). Environmental magnetism and its application towards palaeomonsoon reconstruction. *Jour. Ind. Geophys. Union*, v. 8(1), pp. 1-14.
- Basavaiah, N., Seetharamaiah, J., Appel, E., Juyal, N., Prasad, S., Rao, K.N., Khadkikar, A.S., Nowaczyk, N. and Brauer, A. (2022). Holocene environmental magnetic records of Indian monsoon fluctuations. *Holocene Climate Change and Environment*, pp. 229-247.
- Benn, D.I. and Owen, L.A. (1998). The role of the Indian summer monsoon and the mid-latitude westerlies in Himalayan glaciation: review and speculative discussion. *Jour. Geol. Soc.*, v.155(2), pp.353-363.
- Bhargava, O.N. and Bassi, U.K. (1998). Geology of Spiti-Kinnair Himachal Himalaya. *Geol. Surv. India*, v. 124.
- Bhattacharyya, A., Ranhotra, P.S. and Shah, S.K. (2006). Temporal and spatial variations of late pleistocene-holocene climate of the western himalaya based on pollen records and their implications to monsoon dynamics. *Jour. Geol. Soc. India*, v. 68(3), p. 507.
- Blaauw, M. and Christen, J.A. (2013). Bacon Manual. v2. 3.3. Queens University Belfast, Belfast.
- Bookhagen, B. and Burbank, D.W. (2010). Toward a complete Himalayan hydrological budget: Spatiotemporal distribution of snowmelt and rainfall and their impact on river discharge. *Jour. Geophy. Res.: Earth Surf.*, v. 115(F3).
- Chakraborty, S., Bhattacharya, S.K., Ranhotra, P.S., Bhattacharyya, A. and Bhushan, R. (2006). Palaeoclimatic scenario during Holocene around Sangla valley, Kinnair northwest Himalaya based on multi proxy records. *Curr. Sci.*, v. 91(6), pp. 777-782.
- Chauhan, M.S. (2006). Late Holocene vegetation and climate change in the alpine belt of Himachal Pradesh. *Curr. Sci.*, pp. 1562-1567.
- Chauhan, M.S., Mazari, R.K. and Rajagopalan, G. (2000). Vegetation and climate in upper Spiti region, Himachal Pradesh during late Holocene. *Curr. Sci.*, v. 79(3), pp. 373-377.
- Diwate, P., Khan, F., Maurya, S., Meena, N.K., Humane, S. and Golekar, R.B. (2021). Sedimentation Pattern and its Controlling Factors in Indian Lakes. *Bull. Pure Appl. Sci.-Geol.*,v.40F(1), pp. 38-52.
- Draganits, E., Gier, S., Hofmann, C.C., Janda, C., Bookhagen, B. and Grasemann, B. (2014a). Holocene versus modern catchment erosion rates at 300 MW Baspa II hydroelectric power plant (India, NW Himalaya). *Jour. Asian Earth Sci.*, v. 90, pp. 157-172.
- Draganits, E., Grasemann, B., Janda, C., Hager, C. and Preh, A. (2014b). 300 MW Baspa II—India's largest private hydroelectric facility on top of a rock avalanche-dammed palaeo-lake (NW Himalaya): Regional geology, tectonic setting and seismicity. *Engi. Geol.*, v. 169, pp. 14-29.
- Dutta, S., Mujtaba, S.A.I., Saini, H.S., Chunckekar, R. and Kumar, P. (2018). Geomorphic evolution of glacier-fed Baspa Valley, NW Himalaya: record of Late Quaternary climate change, monsoon dynamics and glacial fluctuations. *Geol. Soc., London*, v. 462(1), pp. 51-72.
- Ganjoo, R.K. and Koul, M.N. (2005). Glacial meltwater impounding: Evidence from the late Quaternary glaciogenic sediments in the Sangla valley, district Kinnaur, Himachal Pradesh, India. *Jour. Earth Syst. Sci.*, v. 114, pp. 381-385.
- Gupta, A.K., Das, M. and Anderson, D.M. (2005). Solar influence on the Indian summer monsoon during the Holocene. *Geophy. Res. Lett.*, v. 32(17).
- Hou, J., D'Andrea, W.J., Wang, M., He, Y. and Liang, J. (2017). Influence of the Indian monsoon and the subtropical jet on climate change on the Tibetan Plateau since the late Pleistocene. *Quat. Sci. Rev.*, v. 163, pp. 84-94.
- Ji, J., Shen, J., Balsam, W., Chen, J., Liu, L. and Liu, X. (2005). Asian monsoon oscillations in the northeastern Qinghai-Tibet Plateau since the late glacial as interpreted from visible reflectance of Qinghai Lake sediments. *Earth and Planet. Sci. Lett.*, v. 233(1-2), pp. 61-70.
- Kaushik, A., Gupta, A.K., Clemens, S.C., Kumar, P., Sanyal, P., Jaiswal, M.K., Maurya, A.S. and Sengupta, S. (2025). Indian monsoon variability during the past 600 years. *Quat. Inter.*, v. 718, p. 109583.
- Khan, F., Meena, N.K., Sundriyal, Y. and Sharma, R. (2022). Indian summer monsoon variability during the last 20 kyr: Evidence from peat record from the Baspa Valley, northwest Himalaya, India. *Jour. Earth Syst. Sci.*, v. 131(3), p. 164.
- Khan, F. (2023). Late Pleistocene to Holocene Paleoclimatic records from Baspa valley and Chakrata North west Himalaya India. Thesis, <http://hdl.handle.net/10603/526347>.
- Liu, Q., Roberts, A.P., Larrasoña, J.C., Banerjee, S.K., Guyodo, Y., Tauxe, L. and Oldfield, F. (2012). Environmental magnetism: principles and applications. *Rev. Geophy.*, v. 50(4).
- Liu, X., Dong, H., Yang, X., Herzschuh, U., Zhang, E., Stuut, J.-B. W., & Wang, Y. (2009). Late Holocene forcing of the Asian winter and summer monsoon as evidenced by proxy records from the northern Qinghai-Tibetan Plateau. *Earth Planet. Sci. Lett.*, v. 280(1-4), pp. 276–284.
- Lone, A.M., Singh, S.P., Shah, R.A., Achyuthan, H., Ahmad, N., Qasim, A., Tripathy, G.R., Samanta, A. and Kumar, P. (2022). The late Holocene hydroclimate variability in the Northwest Himalaya: Sedimentary clues from the Wular Lake, Kashmir Valley. *Jour. Asian Earth Sci.*, v. 229, p. 105184.
- Maurya, S., Rai, S.K., Sharma, C.P., Rawat, S., Chandana, K.R., Dhabi, A.J., Bhushan, R. and Sarangi, S. (2022). Paleo-vegetation and climate variability during the last three millennia in the Ladakh, Himalaya. *Catena*, v. 217, p. 106500.
- Meena, N.K., Diwate, P. and Pandita, S. (2022). Evidence of ENSO and IOD Interplay in Continental Climatic Records from Southern Himalaya (Renuka Lake), India. *Jour. Geosci. Res.*, v. 7, pp. 2455-1953.
- Meena, N.K., Khan, F., Sundriyal, Y., Wasson, R.J., Kumar, P. and Sharma, R. (2024). Holocene paleoclimatic records from Chakrata area, Northwest Himalaya. *Quat. Inter.*, v. 709, pp. 43-54.
- Meena, N.K., Maiti, S. and Srivastava, A. (2011). Discrimination between anthropogenic (pollution) and lithogenic magnetic fraction in urban soils (Delhi, India) using environmental magnetism. *Jour. Appl. Geophy.*, v. 73(2), pp. 121-129.
- Oldfield, F. (1991). Environmental magnetism—a personal perspective. *Quat. Sci. Revi.*, v. 10(1), pp. 73-85.
- Palar, B., Gupta, A.K., Sanyal, P., Kumar, P., Jaiswal, M.K., Singh, R.K., Dash, M.K. and Sharma, R. (2025). Multi-proxy record of monsoon variability since ~1300 CE from Anshupa Lake, Core Monsoon Zone of India. *Palaeogeogr., Palaeoclim., Palaeoeco.*, v. 661, p. 112718.
- Rana, N., Sharma, S., Sundriyal, Y., Kaushik, S., Pradhan, S., Tiwari, G.,

- Khan, F., Sati, S.P. and Juyal, N. (2021a). A preliminary assessment of the 7th February 2021 flashflood in lower Dhauli Ganga valley, Central Himalaya, India. *Jour. Earth Syst. Sci.*, v. 130, pp. 1-10.
- Rana, N., Sundriyal, Y., Sharma, S., Khan, F., Kaushik, S., Chand, P., Bagri, D.S., Sati, S.P. and Juyal, N. (2021b). Hydrological Characteristics of 7 th February 2021 Rishi Ganga Flood: Implication towards Understanding Flood Hazards in Higher Himalaya. *Jour. Geol. Soc. India*, v. 97, pp. 827-835.
- Ranhotra, P.S. and Bhattacharyya, A. (2010). Holocene palaeoclimate and glacier fluctuations within Baspa valley, Kinnaur, Himachal Pradesh. *Jour. Geol. Soc. India*, v. 75, pp. 527-532.
- Ranhotra, P.S., Sharma, J., Bhattacharyya, A., Basavaiah, N. and Dutta, K. (2018). Late Pleistocene-Holocene vegetation and climate from the palaeolake sediments, Rukti valley, Kinnaur, Himachal Himalaya. *Quat. Inter.*, v. 479, pp. 79-89.
- Ranhotra, P.S., Shekhar, M., Roy, I. and Bhattacharyya, A. (2022). Holocene Climate and Glacial Extents in the Gangotri Valley, Garhwal Himalaya, India: A Review. *Climate Change: Impacts, Responses and Sustainability in the Indian Himalaya*, pp. 125-142.
- Rawat, S., Gupta, A.K., Sangode, S.J., Srivastava, P. and Nainwal, H.C. (2015a). Late Pleistocene–Holocene vegetation and Indian summer monsoon record from the Lahaul, northwest Himalaya, India. *Quat. Sci. Rev.*, v. 114, pp. 167-181.
- Rawat, S., Gupta, A.K., Srivastava, P., Sangode, S.J. and Nainwal, H.C. (2015b). A 13,000 year record of environmental magnetic variations in the lake and peat deposits from the Chandra valley, Lahaul: implications to Holocene monsoonal variability in the NW Himalaya. *Palaeogeo., Palaeoclim., Palaeoeco.*, v. 440, pp. 116-127.
- Rawat, V., Rawat, S., Srivastava, P., Negi, P.S., Prakasam, M. and Kotlia, B.S. (2021). Middle Holocene Indian summer monsoon variability and its impact on cultural changes in the Indian subcontinent. *Quat. Sci. Rev.*, v. 255, p. 106825.
- Sagwal, S., Sengupta, D., Kumar, A., Dutt, S., Srivastava, P., Agnihotri, R., Gahlaud, S.K.S., Sarathi Jena, P., Shivam, A. and Bhushan, R. (2023). Late-Holocene wildfire record from the Stagmo peat section, Leh valley, NW Himalaya. *The Holocene*, p. 09596836231157066.
- Sharma, C.P., Rawat, S.L., Srivastava, P., Meena, N.K., Agnihotri, R., Kumar, A., Chahal, P., Gahlaud, S.K.S. and Shukla, U.K. (2020). High-resolution climatic (monsoonal) variability reconstructed from a continuous ~2700-year sediment record from Northwest Himalaya (Ladakh). *The Holocene*, v. 30(3), pp. 441-457.
- Sharma, R., Umapathy, G.R., Kumar, P., Ojha, S., Gargari, S., Joshi, R., Chopra, S. and Kanjilal, D. (2019). Ams and upcoming geochronology facility at inter university accelerator centre (IUAC), New Delhi, India. *Nucl. Inst. and Meth. in Phy. Res. Sec. B: Beam Inter. with Mate. and Atoms*, v. 438, pp. 124-130.
- Shekhar, M.S., Chand, H., Kumar, S., Srinivasan, K. and Ganju, A. (2010). Climate-change studies in the western Himalaya. *Annals Glaci.*, v. 51(54), pp. 105-112.
- Shukla, T., Mehta, M., Dobhal, D.P., Bohra, A., Pratap, B. and Kumar, A. (2020). Late-Holocene climate response and glacial fluctuations revealed by the sediment record of the monsoon-dominated Chorabari Lake, Central Himalaya. *The Holocene*, v. 30(7), pp. 953-965.
- Thompson, R., Stober, J.C., Turner, G.M., Oldfield, F., Bloemendal, J., Dearing, J.A. and Rummery, T.A. (1980). Environmental Applications of Magnetic Measurements. *Science*, v. 207 (4430), pp. 481-486. doi: 10.1126/science.207.4430.481
- Vannay, J.C., Grasemann, B., Rahn, M., Frank, W., Carter, A., Baudraz, V. and Cosca, M. (2004). Miocene to Holocene exhumation of metamorphic crustal wedges in the NW Himalaya: Evidence for tectonic extrusion coupled to fluvial erosion. *Tectonics*, v. 23(1).
- Yang, B., Braeuning, A., Yao, T. and Davis, M.E. (2007). Correlation between the oxygen isotope record from Dasuopu ice core and the Asian Southwest Monsoon during the last millennium. *Quarter. Sci. Rev.*, 26(13-14), pp.1810-1817.